

EXTENDED HIGH-CURRENT ARC DISCHARGES IN AN EXTERNAL MAGNETIC FIELD IN GASEOUS ENVIRONMENTS

© 2025 A. P. Glinov*, A. P. Golovin**, P. V. Kozlov***

Institute of Mechanics, Lomonosov Moscow State University, Moscow, Russia

*e-mail: glshur@imec.msu.ru

**e-mail: gnka_golovin_apsf@mail.ru

***e-mail: kalevala@mail.ru

Received October 07, 2024

Revised March 10, 2025

Accepted March 13, 2025

Abstract. Extended (up to several tens of centimeters) high-current (hundreds of amperes) electric arcs in different gases at atmospheric pressure were experimentally and theoretically investigated. The study of such discharges was carried out on the electric discharge stand of the P-2000 installation of the Institute of Mechanics, Moscow State University. The paper clarifies the data on the influence of an external magnetic field on the stability of such discharges and the formation of branched current channels. One of the areas of the conducted research is the study of the influence of the orientation of the magnetic field imposed on the arc on the processes of discharge development in different gas environments, such as air, CO₂, Ar, N₂. The data for argon and nitrogen are presented most fully. The experiments were carried out in a chamber with transparent walls. The calculation and theoretical study was carried out on the basis of an electrical engineering model using empirical data on the volt-ampere characteristics of arcs between graphite electrodes. It was revealed that the stability of high-current arcs is significantly affected by the dynamics of electrode jets-torches. Traditional models of arcs in an external magnetic field without taking these factors into account show that the direction of the external axial field does not affect the stability of the arcs, affecting only the direction of their twist during the development of helical instability.

Keywords: *extended electric arc, magnetic field, discharge chamber, graphite electrodes, and discharge initiation*

DOI: 10.31857/S10247084250306e2

INTRODUCTION

It is known that high-current extended arc discharges of atmospheric pressure (without special stabilization measures) are unstable and prone to self-extinguishment, as demonstrated, for example, in [1-5]. The adoption of special stabilization measures (imposition of an external magnetic field, stabilization by insulating walls or gas flows, coordination of electrode units, etc.) makes it possible to significantly extend the stability limits of the discharge. This gives a fundamental possibility to use its plasma in some technical appendixes, for example, such as the

anchor of rail gas pedals, or the working medium of other electrophysical installations, for example, plasmatrons. Previously, it was shown at the electrode stand of the laboratory of general hydromechanics of the Institute of Mechanics of MSU that optimization of electrode sliding modes and coordination of electrode assemblies allows to obtain stable arc combustion in an open air atmosphere. This result was provided up to interelectrode distances of 30 cm [6-11]. At the same time, approaches based on data processing of its spectral diagnostics can be used to control plasma characteristics, as for example in [10, 12]. In this work, we present data on research on the stability of extended arcs in discharge chambers due to optimization (selection) of the discharge medium.

PROBLEM FORMULATION

The main experiments were carried out in a discharge chamber (Fig. 1a) with cylindrical side walls made of quartz electrovacuum glass 7 mm thick. The chamber is equipped with a system of Helmholtz rings to create a vertical magnetic field (Fig. 1b). The height and diameter are 250 mm. Vertically oriented discharges were considered. Arcs between graphite (3OPG) electrodes of different diameters (6-150 mm) were investigated. Theoretical modeling of such discharges was carried out in the electrical approximation based on the classical empirical data of G. Ayrton.

The arc discharge is initiated by closing the electrodes under electric voltage and further sliding them to the selected interelectrode gap l_0 (Fig. 2). Typical natural perturbations of the gap caused by imperfection (insufficient tuning) of the system of electromechanical electrode sliding are given in Fig. 3a. In order to conduct special experimental research of the given gap perturbations, a device based on linear modules of milling machines with a programmable law of electrode sliding is used [7]. A characteristic view of the imposed local perturbations is shown in Fig. 36.

The characteristic time of electrode sliding t_0 is 0.1-0.2 s in experiments. The oscillograms of current $I(t)$ and voltage $U(t)$ on the discharge gap were taken synchronously with video images. Pyrometric measurements of the cathode temperature are also carried out with a pyrometer of the DIELTEST type. In general, the extended arc discharge with quasi-stationary currents in a gas medium of atmospheric pressure on graphite electrodes is studied, sometimes in the presence of an external magnetic field provided by a magnetic field system (MS). The electrodes are graphite. Discharge currents are hundreds of amperes, voltages - up to 200 V. The main cathodes are rod cathodes, their diameters $dk = 6-16$ mm, anodes are rods with diameter $da = 16$ mm and rectangular prisms with contact surface $Sa = 600 - 2400$ mm². Theoretical modeling of arcs is a rather complex and difficult task, even within the framework of simplified physical and mathematical models. One of the directions is stability analysis in linear approximation [13, 14], another is direct numerical modeling [15, 16].

THEORETICAL MODELING

Mathematical modeling of electric arc discharge processes (taking into account all significant physical factors) is a very complex and, to date, unsolved problem. This applies both to problem statements and to program-algorithmic developments for them. It should be noted that along with physical processes in the discharge channel itself and the environment, the processes in the electrode, insulators, and external circuit are shafts. A great difficulty arises in the construction and closure of models of charge and neutral particle transport in the boundary zones between heterogeneous media. The problems of accessibility (availability) of databases and the problems of many, widely differing, spatial and temporal scales are also very significant. As a result, researchers in the field of electrophysics are limited to the solution of model problems [17, 18]. It is often faster to perform only experimental research [19].

Among theoretical works devoted to the study of hydrodynamic flows in gaps (without taking into account the flowing currents), we note the work [20]. It considers model automodeling flows of viscous fluid between sliding parallel plates. Mathematically such, even purely hydrodynamic problems, are rather complicated. Therefore, we made an attempt to model the influence of electrode sliding on the stability of combustion of extended high-current arcs not only experimentally, but also on the basis of solutions of problems within the framework of the electrical model under different initial conditions and parameters of the external circuit.

In this work, a simplified electrical engineering modeling approach based on empirical data on arc voltampere approximations is applied [11, 21].

$$L \frac{dl}{dt} = \varepsilon - IR - u(\ell, I) \quad (1)$$

$$u = a + bl + \frac{c + dl}{I} \quad (2)$$

$$\ell = \ell(t) = \begin{cases} V_0 t, & t < t_0 = \ell_0 / V_0 \\ \ell_0 [1 + \alpha \exp(-\gamma(t - t_0)) \sin \omega(t - t_0)], & t \geq t_0 \end{cases} \quad (3)$$

In these formulas: (1) - Kirchhoff equation, (2) - arc voltage dip U in the interelectrode gap l (the so-called H. Ayrton approximation [21]). Formula (3) is a given form of change of the gap l with time t . This form is empirical, based on processing and approximation of our long-term experimental data, was given earlier for calculations in [10]. The values L, R, I and ε are the inductor, ballast resistance, discharge current and EMF of its power supply, respectively. The model parameter: $V_0 = \text{const}$ is the rate of electrode sliding to the required distance (gap) l_0 . The constants H. Ayrton (a, b, c, d) depend primarily on the discharge medium and electrode materials.

The parameters γ , ω and α are decrement, frequency and amplitude of oscillations of the interelectrode gap from its "working" (stationary) value l_0 .

In Fig. 4 gives dimensionless time dependences of the gap, current and voltage.

The scales of current, voltage, gap and time unmeasuring are as follows:

$$I_* = \frac{I_m}{R}, \quad U_* = \varepsilon, \quad l_* = l_0, \quad t_* = t_0$$

The base case curves (1), meet the following parameters:

$$\begin{aligned} \frac{a}{\varepsilon} &= 0.1, \quad \frac{\omega l_0}{V_0} = 5, \quad \frac{b l_0}{\varepsilon} = 0.5 \\ \frac{\gamma l_0}{V_0} &= 1, \quad \frac{l_0 R}{V_0 L} = 2 \times 10^5, \quad \frac{d l_0}{c} = 60 \\ \frac{c R}{\varepsilon} &= 1.7 \times 10^{-4}, \quad \alpha = 0.5 \end{aligned}$$

The interelectrode distance (l), discharge current (I) and voltage (U) are shown in Fig. 4a, c, respectively. Variations of the EMF parameter are marked by the set of curves (1-3). It is of key importance for the stability of arc burning at increasing the technical reliability of the sliding system. Then (at ensuring this reliability) the corresponding parameter is negligibly small: $\alpha \ll 1$. In particular, the variant corresponding to curves (3) shows an example of arc self-extinguishing at insufficient EMF to maintain discharge. As noted in [7], as well as on the basis of experimental data of this work, large-scale perturbations of the gap ($l' = l - l_0$) of 10% or more from its stationary value l_0 are also very dangerous, as well as insufficient EMF.

EXPERIMENTAL RESULTS

Unless otherwise specified, experiments in this work are performed with an ideally (rigidly) stabilized electrode sliding system ($\alpha = 0$ when a given steady-state gap l_0) is reached.

Different gases were considered for the interelectrode medium: air and some of its important components for technical appendixes: argon, nitrogen, carbon dioxide. It turned out that of the gases considered, argon is preferable (see Fig. 5, 6). It requires less voltage dips and provides more stable combustion. However, its ionization potential is higher than that of its competitors, the gases considered. Possibly, the advantages of argon are due to the greater stability of the argon plasma cathode jet and somewhat greater evaporation of the graphite cathode material in an argon environment. Graphite has a lower ionization potential than argon. Further computational-theoretical and experimental research is needed to clarify the results. Some estimates of hydrodynamic characteristics of electrode plumes are given in Table 1.

Here, the Reynolds number was estimated using the formula

$$Re = \frac{\rho V \delta}{\mu}$$

The values ρ_0 , μ_0 are the density and dynamic toughness of the flare medium at atmospheric pressure and temperature $T_0 = 300K$. The temperature $T = 6kK$. The velocity V is of the order of 10 m/s. Effective (average) diameter $\delta = 6$ mm. Usually in experiments of recent years on P2000, the Re number is in the range of 0.5-5.

The toughness was estimated using the polytropic law [22]

$$\mu = \mu_0 \left(\frac{T}{T_0} \right)^n, \quad n = 0.76$$

Reference books [23, 24] were used to compile Table 1.

The effect of the amplitude of the gap perturbations is shown in Fig. 7.

It can be seen that perturbations of the gap (l_0) of 10% or more of l_0 are very dangerous (see Fig. 7c-f). They cause sharply unsteady oscillations of large amplitude of current and voltage throughout the discharge time. At the same time, the shape of the arc current column and electrode flares is also unstable.

A summary data set of experimental results without imposing an external magnetic field on the discharge is presented in Table 2.

As can be seen, argon medium is capable of providing atmospheric pressure discharge stability at significantly lower applied electrical voltages and discharge gaps than other gas media.

In Table 2, the active surfaces of the anode and cathode (Sa and Sk), current and voltage dip across the discharge gap (I , U), and gap (l) are labeled.

The influence of the orientation of the external axial magnetic field in different gases is characterized in Figs. 8-12. These figures trace in sufficient detail the dynamics of changes in the shape of the arc column and electrode flares. The detailed presentation of the frames is due to the desire to trace the most tangible effects of the magnetic field orientation.

However, as follows from the detailed video frames of the discharge, the effects of imposing a longitudinal magnetic field on the vertical discharge associated with the change of its direction are rather weak. As an example, the results of experiments in argon medium are given. In these experiments, the effect of superposition of the magnetic field and change of its polarity on the discharge combustion is most noticeable.

The authors are particularly interested in the discharge in CO₂ gas, both as one of the constituent elements of the air environment and as a product of its pollution due to the rapid growth of the world economy.

The calculated emission level for the CO₂ plasma at $T = 10\ 000^\circ\text{K}$ strongly exceeded the values of the experiment data. The calculated spectrum for the temperature of 6000°K was closest to the experiment data. Spectral measurements were carried out at 5 mm from the cathode according to the method described in [10].

The largest discrepancies between the data of the computational model and experiment are recorded in the red region of the spectra. Here, the level of the solid spectrum increases compared to the linear composition of the spectrum. The reason for this may be the emission of hot graphite particles (solid phase) located in the cathode jet as a result of its erosion.

Experimental spectra in which atomic oxygen (O) and carbon (C) lines appeared are shown in Fig. 13.

Calculations of the spectra of the discharge medium were performed using the program and database [25].

It can be seen that atomic oxygen and carbon are present in the discharge gap. But the reason for their appearance in the discharge gap may be not only the collapse of CO₂ molecules, but also the erosion of the graphite 3OPG cathode and the escape of pre-captured air from its pores. Therefore, nothing can be said yet about the efficiency of utilization of CO₂ by arc discharge. The question requires further research.

CONCLUSION

A modular discharge chamber with transparent lateral cylindrical walls made of quartz electrovacuum glass for gaseous media at atmospheric pressure has been manufactured and experimentally tested. The chamber is designed for high-current quasi-stationary discharges up to currents and voltages of hundreds of amperes and volts, respectively.

Both computational-theoretical and experimental research of the processes of initiation, stabilization and extinguishing of extended high-current electric arcs was carried out in this chamber.

Quasi-stationary discharges in air, nitrogen, argon, and carbon dioxide have been studied. Theoretical modeling of arcs is carried out in the electrical engineering approximation on the basis of classical empirical data on volt-ampere characteristics of arcs between graphite electrodes.

The dynamics of electrically conductive gases in the discharge gap is traced experimentally. The possibilities of increasing stabilization of initiation and combustion of arc discharges due to the choice of discharge medium are shown. The conclusions of our previous works on the necessity of coordination of electrode assemblies are confirmed. It is confirmed that the flow of electric current significantly depends on the interelectrode medium. The necessity of optimization of electrode opening rate, their size and shape when working out discharge systems for quasi-stationary atmospheric pressure arcs is noted. The optimal gas (argon) for research of atmospheric pressure discharges at moderate power of current sources (~ 100 kW) has been determined.

The results obtained in this work may be in demand:

- for modeling tests of protective coatings of aircraft during their entry into dense layers of the planets' atmospheres;
- in the development of systems for initiation and extinguishing of extended electric arcs;
- for the development of facilities for the utilization of toxic wastes that are difficult to decompose using traditional chemical technologies;
- in the development of technologies for plasma spraying (for example, graphite) powders on material surfaces.

The results were partially reported at the 50th International (Zvenigorod) Conference on Plasma Physics and UTS [26] and the XIII All-Russian Congress on Theoretical and Applied Mechanics [27].

FUNDING

The work was carried out in accordance with the research plan of the Lomonosov Moscow State University Research Institute of Mechanics, partially funded by RFBR grant No. 18-29-21022.

REFERENCES

1. *Finkelnburg W., Mecker G.* Electric arcs and thermal plasma. MOSCOW: IL, 1961.
2. *Raiser Yu.P.* Physics of gas discharge. Moscow: Nauka, 1987. 592 p.
3. *Zhukov M.F., Koroteev A.S., Uryukov B.A.* Applied dynamics of thermal plasma. Novosibirsk: Nauka, 1975. 296 p.

4. *German V.O., Glinov A.P., Golovin A.P., Kozlov P. V., and Lyubimov G.A.* Some Features of Imaging of the Processes Occurring in an Extended Arc Discharge in Atmospheric Pressure Air // *Plasma Physics Reports*. 2013. V. 39. N. 13. P. 1142–1148.
5. *German V.O., Glinov A.P., Kozlov P.V., and Lyubimov G.A.* Effect of the Design Parameters and the Atmosphere Composition on the Electric Discharge Shape // *Fluid Dynamics*. 2011. V. 46. N. 6. P. 958–966.
6. *Glinov A.P., Golovin A.P., Kozlov P.V., Shaleev K.V., Lyubimov G.A.* Study of arc discharges on the P-2000 facility. // *J. Phys.: Conf.* 2019. Ser. 1250 012019. doi:10.1088/1742-6596/1250/1/012019
7. *Glinov A.P., Golovin A.P., and Kozlov P.V.* Studies of initiation and quenching of extensive high-current discharges // *J. Phys.: Conf.* 2021. Ser. 2055 012006. doi:10.1088/1742-6596/2055/1/012006
8. *Glinov A.P., Golovin A.P., Kozlov P.V.* Optimization of jet plasma flows in an external magnetic field// *Applied Physics*. 2017. № 6. P. 26-32.
9. *Glinov, A.P.; Golovin, A.P.; Shaleev, K.V.* Influence of the external magnetic field on the stability of the extended arc discharge and the formation of multichannel current structures // *Applied Physics*. 2018. № 2. P. 21-28.
10. *Glinov A.P., Golovin A.P., Kozlov P.V.* Study of initiation of arc discharges by opening of initially closed electrodes // *Physico-chemical kinetics in gas dynamics*, Moscow State University Research Institute of Mechanics Publishing House (Moscow, 2020), V. 21, No. 2. DOI: <http://doi.org/10.33257/PhChGD.21.2.916>
11. *Glinov A.P., Golovin A.P., Kozlov P.V., Shaleev K.V.* Dynamics of the electric arc shape and associated magnetogasdodynamic currents, arising at opening of initially closed electrodes // *Physico-chemical kinetics in gas dynamics*, published by the Research Institute of Mechanics of Moscow State University (Moscow, 2019). V. 20. N. 2. DOI: <http://doi.org/10.33257/PhChGD.20.2.835>
12. *German V.O., Glinov A.P., Kozlov P.V., Lyubimov G.A.* Spectral Properties of a Diffuse-Constricted Arc Discharge // *High Temperature*. 2012. V. 50. N. 2. P. 167-177.
13. *Glinov A.P.* Stability of Conducting Medium Flows between Plane Continuous Electrodes Inclined to the Horizon. // *Fluid Dynamics*. 2015. V. 50. N. 3. P. 322-331.

14. *Glinov A.P.* Two-Dimensional Analysis of the Stability of Conducting Medium Flows between Permeable Plane Electrodes Inclined to the Horizon. // *Fluid Dynamics*. 2015. V. 50. № 4 P. 483-493.
15. *Vasiliev, E.N.; Nesterov, D.A.* Computational modeling of interaction of an electric arc with a gas flow (in Russian) // *Izv. RAS. MZHG*. 2013. № 2. P. 126-136.
16. *Urusov R. M., Urusova I. R.* Numerical modeling of the helical shape of an electric arc in an external axial magnetic field. // *TVT*. 2017. V. 55. V. 5. P. 661-668.
17. *Nedospasov A.V., Khait V.D.* Fundamentals of physics of processes in devices with low-temperature plasma. M.: Energoatomizdat, 1991. 224 p.
18. *Zhukov M.F., Koroteev A.S.* Theory of thermal electric arc plasma. Ч. 1,2. Novosibirsk: SO Nauka, 1987. 576 p.
19. *Bron O.B., Sushkov L.K.* Plasma flows in the electric arc of switching devices. L.: Energia, 1975. 212 p.
20. *Petrov, A.G.* Exact solution of the equations of the axisymmetric motion of a viscous fluid between parallel planes at their convergence and sliding // *Izv. RAS. MZHG*. 2019. № 1. P. 58-67.
21. *Ayrton H.* The Electric Arc.", The Electrician Series, D. Van Nostrand Company, Inc., N.Y., 1902. p. 120-130.
22. *Loytsyansky L. G.* Mechanics of Fluid and Gas. Moscow: Nauka, 1973. 736 p.
23. *Grigoriev I.S., Meilikhov E.Z.* Physical quantities. Reference book. Moscow: Energoatomizdat, 1991. 1234 p.
24. *Kuhling H.* Handbook of Physics. Moscow: Mir, 1982. 519 p.
25. *Akimov Y.V., Bykova N.G., Zabelinsky I.E., Kozlov P.V., Levashov V.Y., Gerasimov G.Ya.* Program for calculation of spectra of two-atom molecules "SPECTR" // Certificate of registration of rights to software, database № 2023687422 from December 14, 2023.
26. *Glinov A.P., Golovin A.P., Kozlov P.V.* Features of combustion of extended high-current arcs in an external magnetic field in different gas media // L International (Zvenigorod) Conference on Plasma Physics and STS, March 20-24, 2023, ICPAF-2023. Coll. of abstracts, M: PLASMAIOPHAN 2023, P. 231.

27. Glinov A.P., Golovin A.P., Kozlov P.V. Research of initiation and current flow and interelectrode medium of different atmospheric pressure gases in extended discharge chambers. // XIII All-Russian Congress on Theoretical and Applied Mechanics / Collection of abstracts. report. in 4 T. August 21-25, 2023, St. Petersburg. T. 2. Mechanics of liquid and gas. Peter the Great St. Petersburg Polytechnic University. St. Petersburg 2023. P. 743-745.

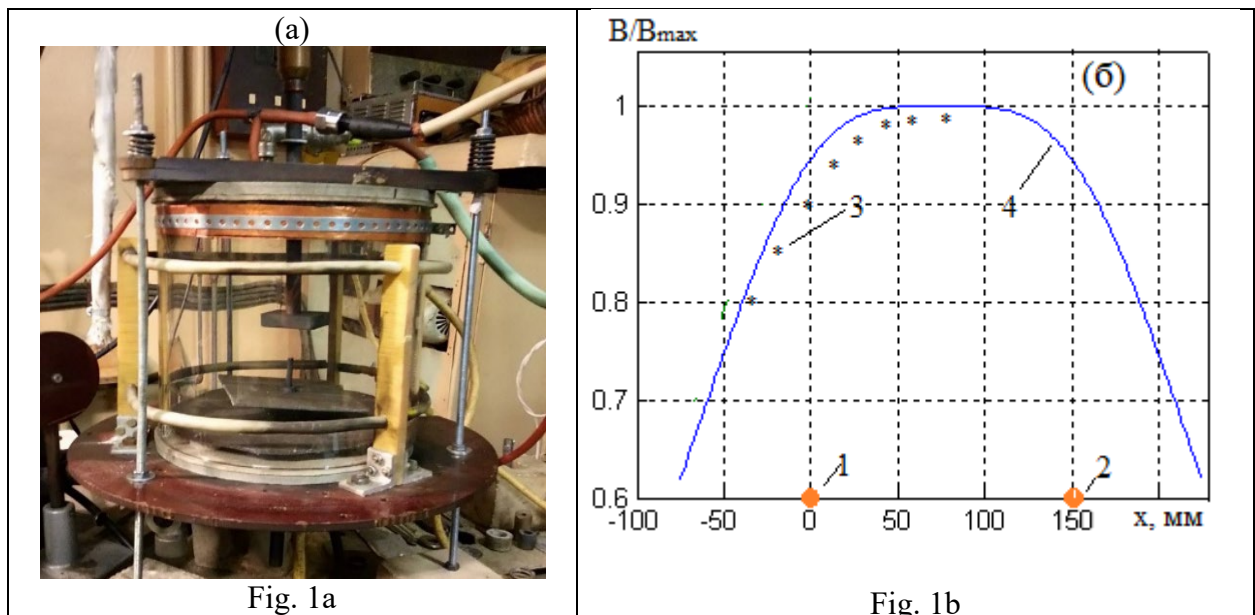


Fig. 1.

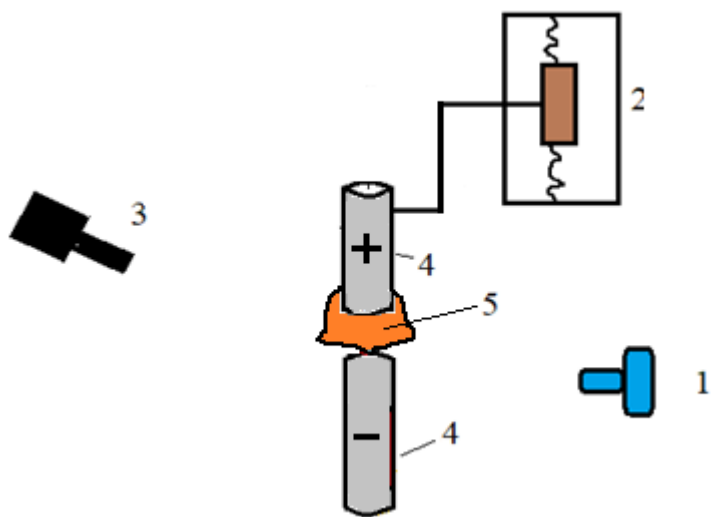


Fig. 2.

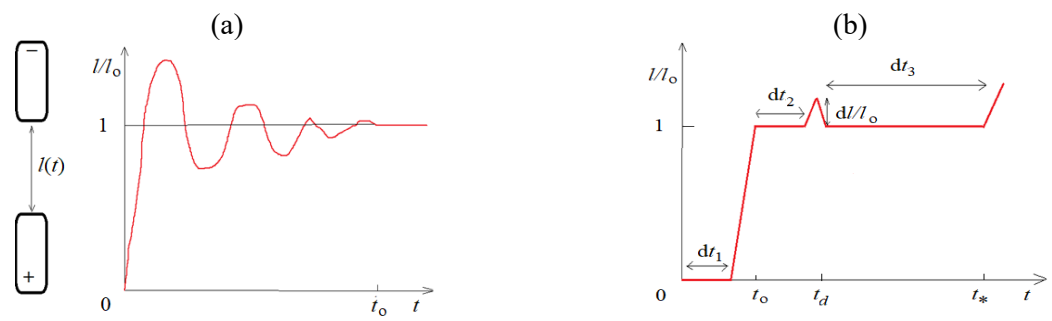
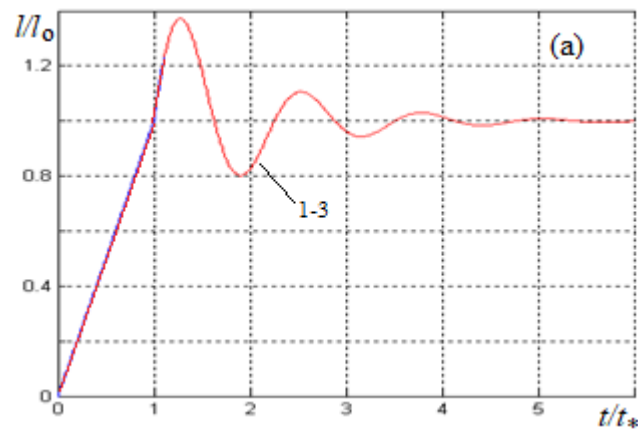


Fig. 3.



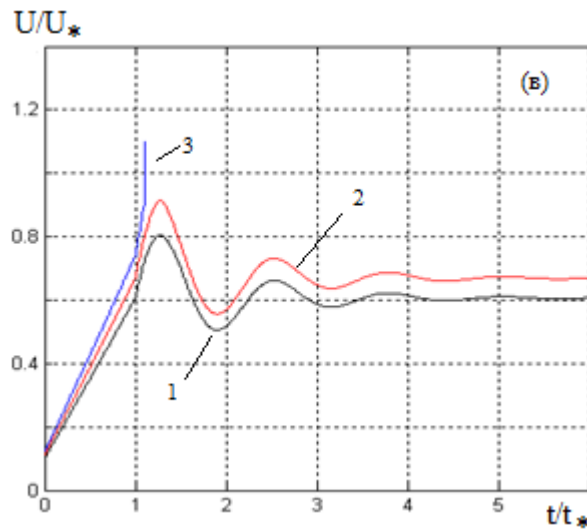
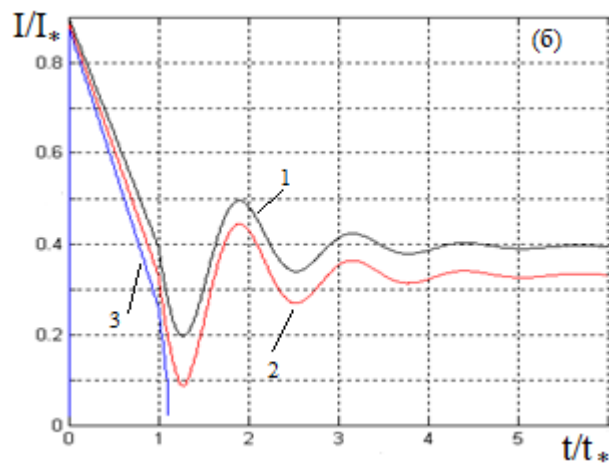


Fig. 4.

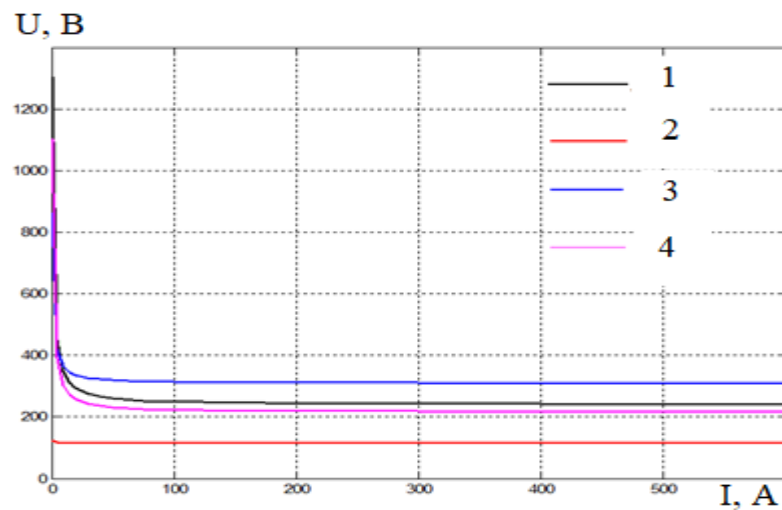
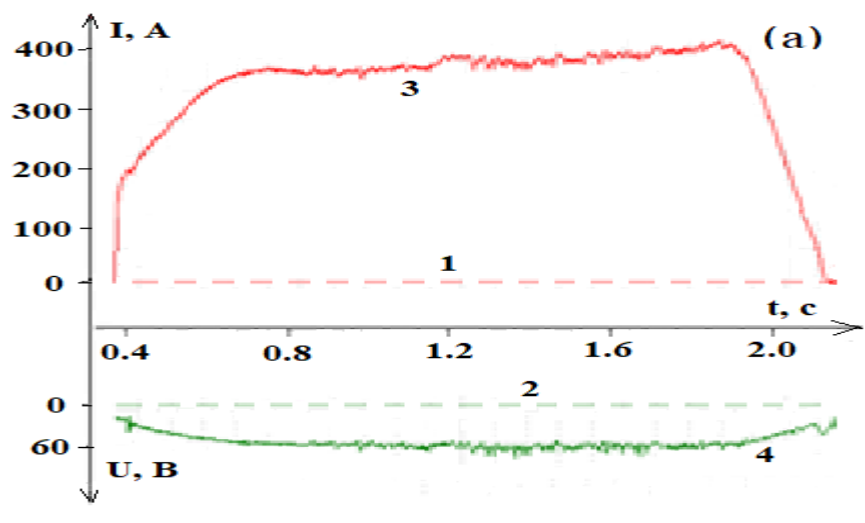


Fig. 5.



(б)
Кадр 469, $t = 0.39$ с



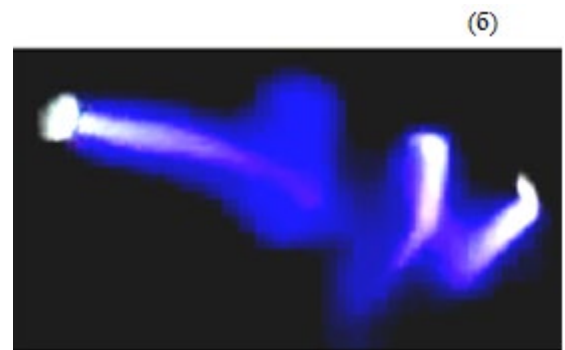
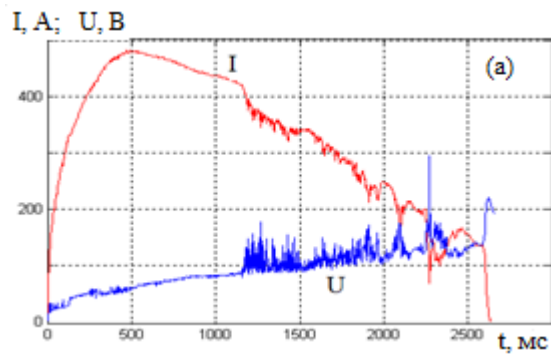
Кадр 897, $t = 0.75$ с



Кадр 1664, $t = 1.39$ с



Fig. 6.



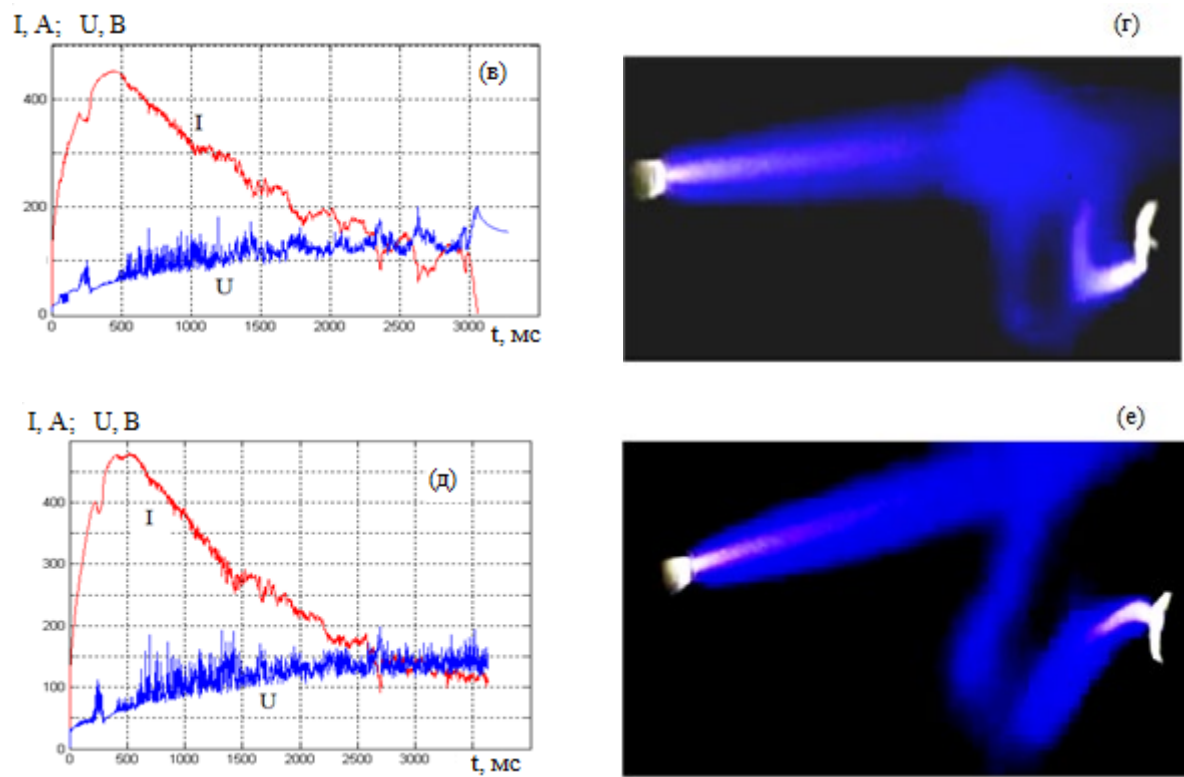


Fig. 7.

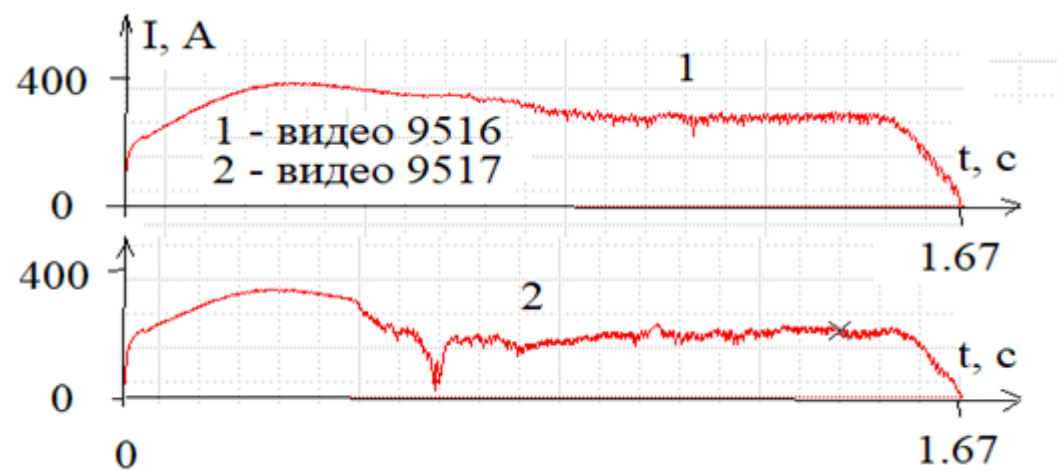


Fig. 8.

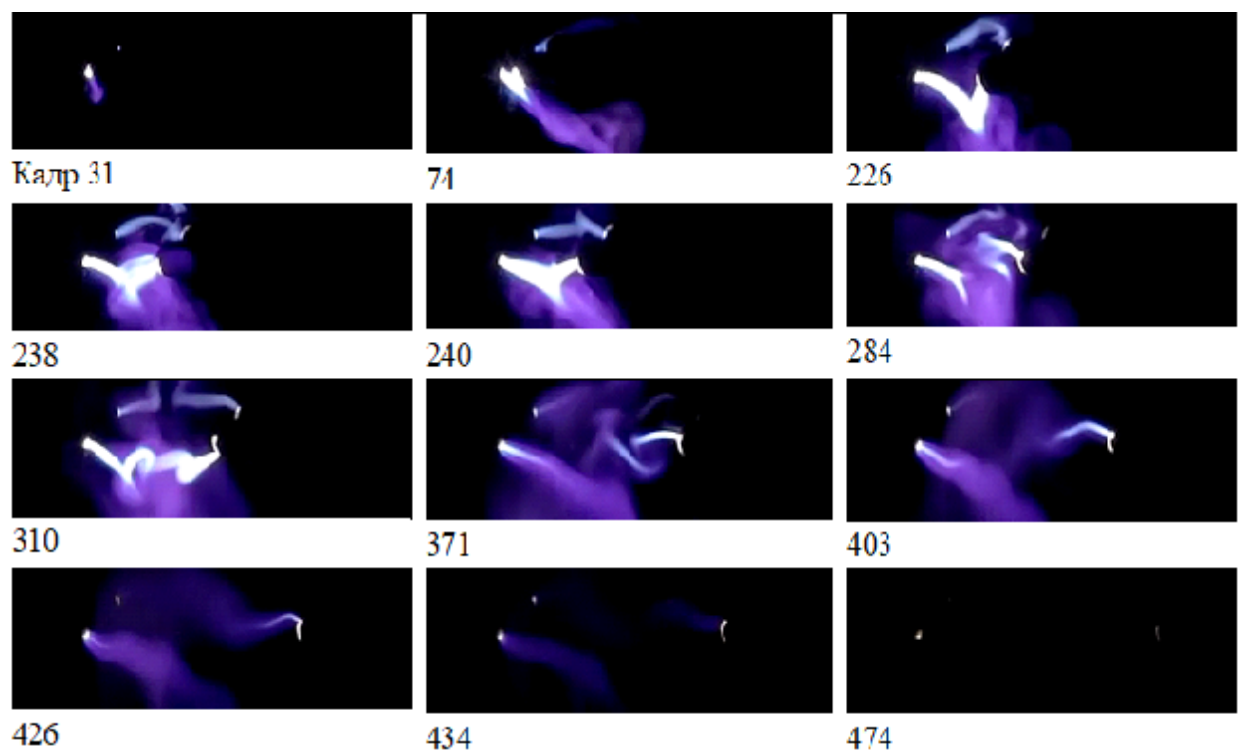


Fig. 9.

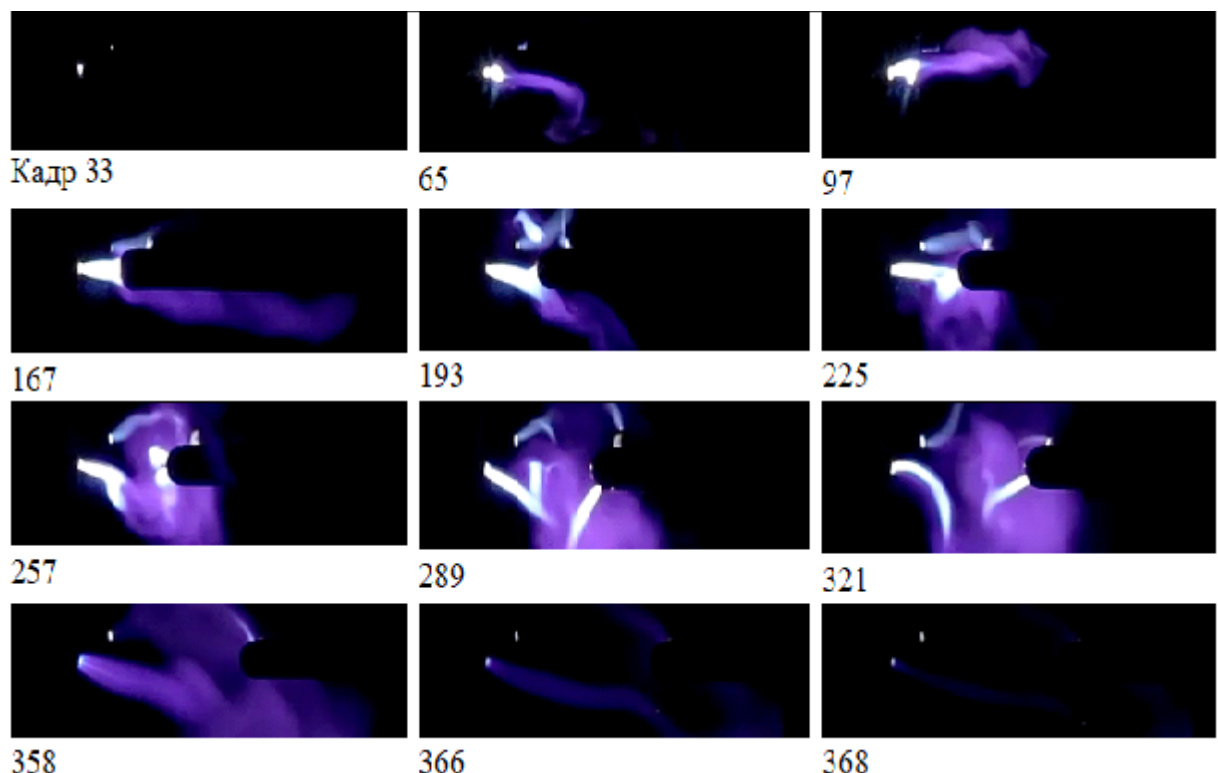


Fig. 10.

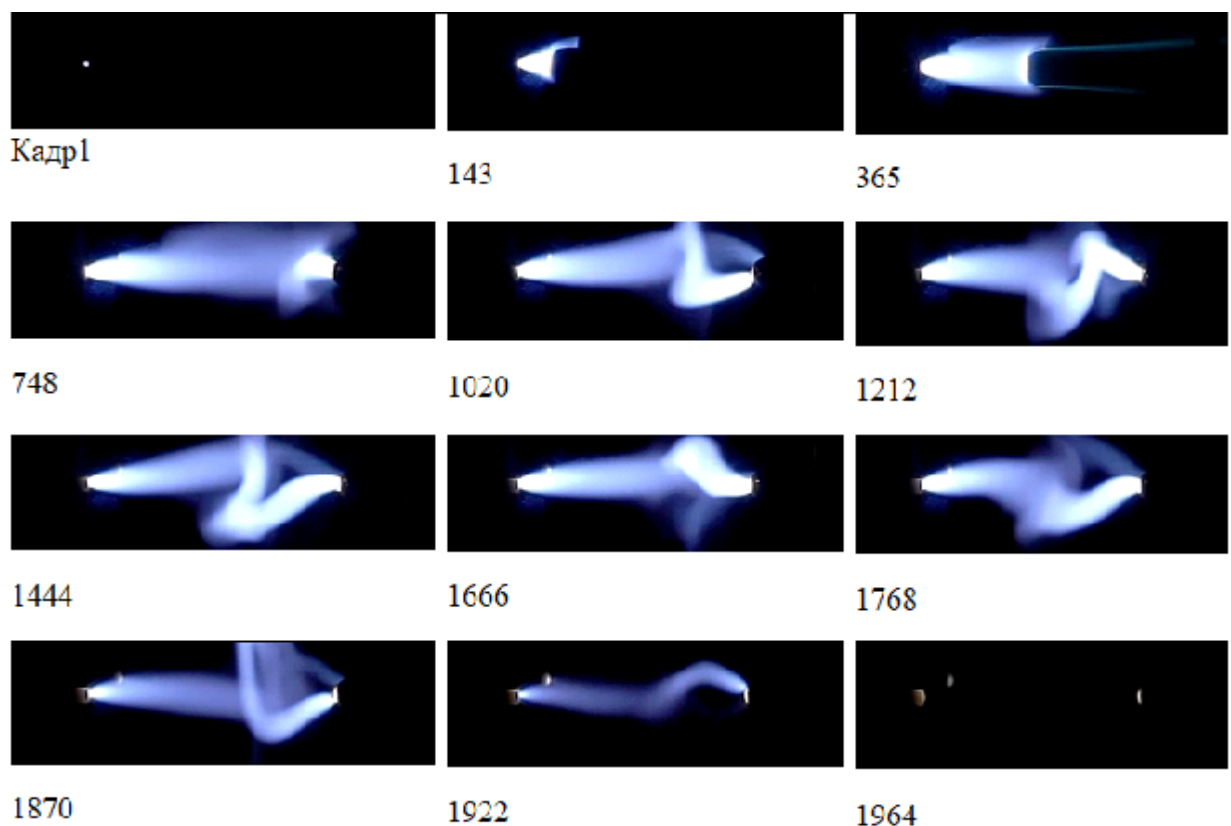


Fig. 11.

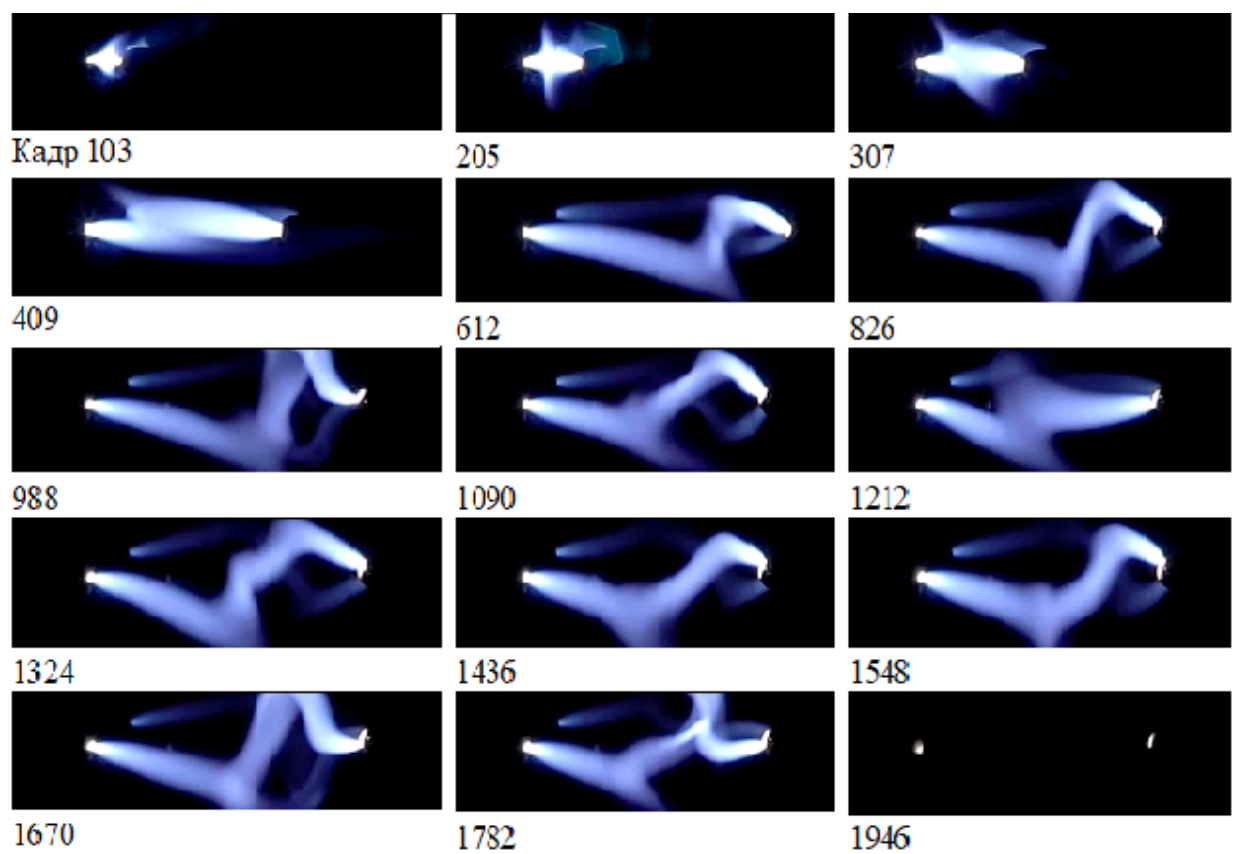


Fig. 12.

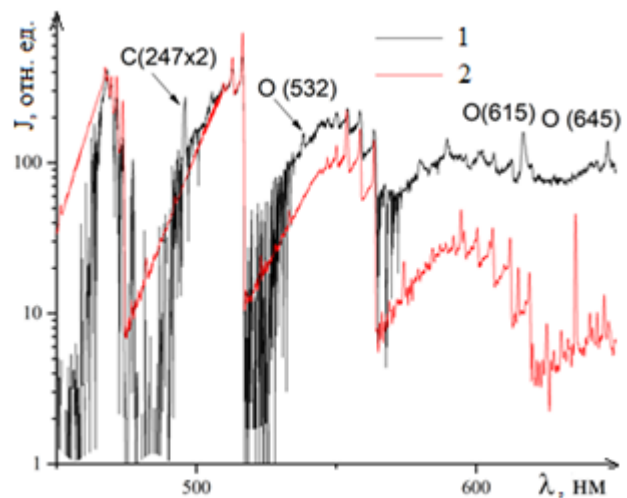


Fig. 13.

FIGURE CAPTIONS

Fig. 1. Discharge chamber with a magnetic system in the form of two Helmholtz rings (a) and distribution of the axial magnetic field of the coil along the vertical axis x : 1, 2 - coil rings; 3, 4 - experimental and calculated data, respectively.

Fig. 2. - scheme of discharge initiation and its visualization and pyrometry: 1 - video camera, 2 - electrode sliding mechanism, 3 - pyrometer, 4 - electrodes, 5 - arc

Fig. 3. Qualitative picture of the evolution of ${}^{\circ}$ of the electrode gap at unbalanced or moderate stabilization of the system of electrode sliding on the drive from printers (a) and - programmable drive on the linear module of the milling machine with imposition (if necessary) of the gap perturbations (b): dt_1 - dt_3 - set time intervals; t_0 , t_d , t^* - times of sliding, localization of disturbances, start of arc extinguishing.

Fig. 4. Effect of normalized EMF(ε), dimensionless: gap (a), current (b), voltage (c); base case $\varepsilon = \varepsilon_b$ (1); $\varepsilon_b / 1.1$ (2); $\varepsilon_b / 1.1^2$ (3)

Fig. 5. Voltampere characteristics of arcs between graphite electrodes in different gases calculated by the model [21]: air (1), nitrogen N_2 (2), argon Ar (3), carbon dioxide CO_2 (4).

Fig. 6. Stabilization of discharge in argon medium: oscillograms of current and voltage (a) and video frames (b) at the indicated moments of time t ; gap $l_0 = 50$ mm, video recording frequency $f = 1200$ fps

Fig. 7. Effect of the gap perturbation amplitude ($l' - l_0$) on the discharge stability in the air medium of atmospheric pressure: oscillograms of current I and voltage U (a, c, e) and corresponding typical video frames (b, d, f): $l_0 = 100$ mm; $(l' - l_0) / l_0 = 0\%$ (a, b), 10% (c, d), 50% (e, f). In the video frames the current $I = 135A$ (b), $120A$ (d), $130A$ (e).

Fig. 8. Discharge current curves in argon of atmospheric pressure: magnetic field B and current I are directed opposite (1) and in the same direction (2)

Fig. 9. Video frames of vertical discharge in nitrogen in an axial magnetic field: movie 9508, $f = 1200$ fps, $p = 1$ atm, magnetic field $B = 12$ mTl against the direction of current I ; gap $l_0 = 100$ mm, $U_{xx} = 170$ B

Fig. 10. Video frames of vertical discharge in nitrogen in an axial magnetic field: Film 9520, $f = 1200$ fps, $p = 1$ atm, magnetic field $B = 12$ mTl along the direction of current I ; gap $l_0 = 100$ mm, $U_{xx} = 170$ B

Fig. 11. Video frames of vertical discharge in argon in an axial magnetic field: movie 9517, $f = 1200$ fps, $p = 1$ atm, magnetic field $B = 12$ mTl along the direction of current I ; gap $l_0 = 100$ mm, $U_{xx} = 110$ B

Fig. 12. Video frames of vertical discharge in argon in an axial magnetic field: movie 9516, $f = 1200$ fps, $p = 1$ atm, magnetic field $B = 12$ mTl against the direction of current I ; gap $l_0 = 100$ mm, $U_{xx} = 110$ B

Fig. 13. Radiation intensity in relative units in a gas discharge cord of atmospheric pressure in CO_2 at a distance of 5 mm from a graphite cathode: Swann bands of carbon molecule (C_2), atomic lines of oxygen (O) and carbon (C - second order 247 nm); 1 - data of our experiments, 2 - calculation at temperature $T = 6kK$

Table 1

Parameters	Air	Ar	N ₂	CO ₂	He	O ₂
ρ_0 , kg/m ³	1.29	1.784	1.25	1.98	0.179	1.47
μ_0 , mPa s	0.0182	0.02108	0.0175	0.147	0.0196	0.0202
Re	0.4364	0.5211	0.4398	0.8293	0.0562	0.4482

Table 2

Start	S_a , mm ²	S_k , mm ²	U _{XX}	I, A	U, B	Duration discharge, with	Gas	d, mm	Arc stability
1	600	150	130	230	118	0.6	N ₂	90	<i>U_{XX} insufficiency suppression</i>
2	600	150	150	414	190	0.8	N ₂	-	- (no)
3	600	150	170	488	107	1.7	N ₂	-	+ (is)
4	600	150	180	505	89	1.8	N ₂	-	+
5	600	150	100	165	56	0.3	CO ₂	-	-
6	600	150	150	400	86	0.3	CO ₂	-	-
7	600	150	170	340	56	0.15	CO ₂	-	-
8	600	150	90	150	30	0.23	CO ₂	-	-
9	600	150	90	200	65	0.46	Ar	-	<i>instability during current drop</i>
10	600	150	110	246	68	0.45	Ar	-	<i>instability during current drop</i>
11	600	150	130	448	69	1.8	Ar	-	+
12	600	150	120	390	67	1.9	Ar	-	<i>instability during current drop</i>
13	2400	150	70	164	49	2.0	Ar	-	+
14	2400	150	50	65	17	0.4	Ar	-	-
15	2400	150	60	129	44	0.6	Ar	-	-
16	2400	150	70	127	56	1.9	Ar	-	+
17	2400	150	60	118	50	0.55	Ar	-	-
18	2400	150	100	186	83	0.36	CO ₂	-	-